Earth and Space Science

RESEARCH ARTICLE
10.1029/2019EA000652

Special Section:
Results from the Initial NASA Solar Irradiance Science Team (SIST) Program

A Revised Magnesium II Core-to-Wing Ratio From SORCE SOLSTICE

M. Snow[1], J. Machol[2,3], R. Viereck[2,4], T. Woods[1], M. Weber[5], D. Woodraska[1], and J. Elliott[1]

[1]LASP, University of Colorado Boulder, Boulder, CO, USA, [2]CIRES, University of Colorado Boulder, Boulder, CO, USA, [3]NOAA National Centers for Environmental Information, Boulder, CO, USA, [4]NOAA Space Weather Prediction Center, Boulder, CO, USA, [5]Institute of Environmental Physics, University of Bremen, Bremen, Germany

Abstract The Magnesium II core-to-wing ratio (also known as the Mg II index) is a widely used proxy for ultraviolet solar spectral irradiance variability. We have developed a new algorithm for calculating this index from the SOLar-STellar Irradiance Comparison Experiment (SOLSTICE) on the SOlar Radiation and Climate Experiment (SORCE). The new method uses weighted sums of the core and wing regions of the spectrum calculated from the daily level three high-resolution spectrum. We also describe a new method of scaling the results in order to compare to other measurements. This new method scales each data set to a standard spectral resolution rather than scaling to other data sets during periods of overlapping measurements. Finally, we quantify the effect of long-term instrument degradation on the Mg II index. In the case of SORCE SOLSTICE, using uncorrected data would produce an error of less than 0.6% of the solar cycle amplitude over a decade.

Key Points:
- We have developed a revised algorithm for calculating the Mg II index from SORCE
- We describe a new method for scaling Mg II data sets from different instruments
- We analyze the effect of long-term instrument degradation on the Mg II index

Correspondence to:
M. Snow,
snow@lasp.colorado.edu

Citation:
Snow, M., Machol, J., Viereck, R., Woods, T., Weber, M., Woodraska, D., & Elliott, J. (2019). A revised Magnesium II core-to-wing ratio from SORCE SOLSTICE. *Earth and Space Science*, *2*, 2106–2114. https://doi.org/10.1029/2019EA000652

Received 31 MAR 2019
Accepted 28 SEP 2019
Accepted article online 31 OCT 2019
Published online 16 NOV 2019

1. Introduction

Variation in the solar spectral irradiance (SSI) drives short timescale changes in the middle atmosphere of the Earth, and on longer timescales it influences the Earth's climate (Floyd et al., 2002). In particular, changes in the 200- to 300-nm region of the solar spectrum control the creation and destruction of ozone (Haigh, 1994; Heath & Schlesinger, 1986). Accurate measurements of SSI variation are also needed to predict the density of the thermosphere for satellite orbit drag calculations (Thuillier & Bruinsma, 2001), as well as modeling the atmosphere in a variety of contexts (Thuillier et al., 2012).

Heath and Schlesinger (1986) defined an easily measured proxy for solar magnetic activity using the feature in the solar spectrum near 280 nm produced by ionized magnesium (i.e., Mg II h and k lines). The ratio of the irradiance in the cores of these wide absorption lines to the irradiance in the nearby continua on either side produces a unitless quantity that is highly correlated to SSI variability throughout the ultraviolet. One of the primary advantages of such a relative measurement—rather than an absolute measurement—is that most instrument artifacts that affect both core and wings will cancel out. Section 4 is devoted to analysis of the residual effect of long-term instrument degradation on the Mg II index. Dudok de Wit et al. (2009) compared nine different proxies for solar activity to determine their efficiency and determined that the Mg II index gave the best global performance as a predictor of SSI variability. Therefore, understanding the natural and artificial sources of variability in the Mg II index is essential for understanding the Sun's role in the long- and short-term variability of the atmosphere and climate.

2. Characteristics of the Magnesium II Index

2.1. Observational Record

The Mg II index has the luxury of a long history of daily measurements, as well as several published long-term composites. The most recent description of the algorithm for constructing such a composite is Viereck et al. (2004). The Viereck et al. (2004) composite includes data up to the beginning of the SOlar Radiation and Climate Experiment (SORCE; Rottman, 2005). From 1978 to 1991, the Mg II index was only measured by low-resolution instruments with once per day time cadence. During the 1990s, observations from moderate-resolution instruments became available, often with several measurements per day. Since 2003, higher spectral resolution observations have become more common. As shown in Snow, McClintock, Woods, et al. (2005) and Snow and McClintock (2005), the Mg II index shows solar variability on short

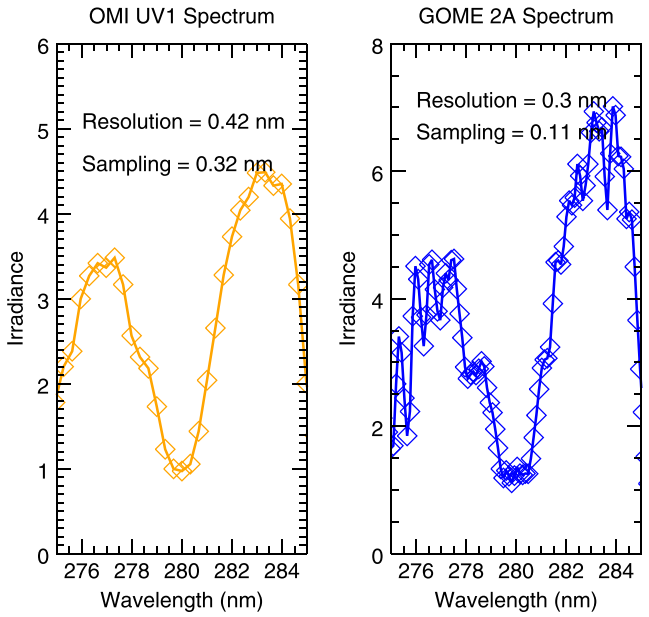

Figure 1. Typical spectrum from (left) OMI and (right) GOME-2A. Irradiance units are watts per square meter per nanometer. GOME = Global Ozone Monitoring Experiment; OMI = Ozone Monitoring Instrument.

timescales, and the higher spectral resolution observations allow for higher signal-to-noise measurements of that variability.

2.1.1. Classic Observations

The core-to-wing ratio first described by Heath and Schlesinger (1986) was for a low spectral resolution (1.1 nm) instrument. The Solar Ultraviolet Backscatter Radiometer (SBUV and SBUV/2; Heath et al., 1975; Frederick et al., 1986) has been making daily SSI measurements from 1978 onward, including the currently operating NOAA19 instrument launched in 2009. For such an instrument, the core is measured at 279.8, 280.0, and 280.2 nm. The continuum wavelengths are 276.6, 276.8, 283.2, and 283.4 nm. The definition of the proxy, P_{MgII}, is given by

$$P_{\mathrm{MgII}} = \left(\frac{4}{3}\right) \frac{I_{279.8} + I_{280.0} + I_{280.2}}{I_{276.6} + I_{276.8} + I_{283.2} + I_{283.4}}. \quad (1)$$

The solar spectrum from an SBUV-type instrument is not observed directly. The incoming solar irradiance is reflected off a diffuser plate into the instrument (DeLand et al., 2004). Careful analysis of the geometry of this reflection is required to produce a daily solar spectrum.

2.1.2. Moderate Spectral Resolution Observations

Starting with the launch of the Upper Atmosphere Research Experiment (UARS) in 1991, instruments with higher spectral resolution began making daily SSI measurements near 280 nm. The SOLar-STellar Irradiance Comparison Experiment (SOLSTICE; Rottman et al., 1993) has a spectral resolution of 0.3 nm and takes two samples per slit width. Floyd et al. (1999) describe construction of a Mg II index from UARS Solar Ultraviolet Spectral Irradiance Monitor observations.

The Ozone Monitoring Instrument (OMI; Levelt et al., 2006) has been making daily measurements of SSI, including the 280-nm range, since 2004. The spectral resolution in this region is 0.5 nm, and the daily Mg II index is available online (https://sbuv2.gsfc.nasa.gov/solar/omi/). A typical spectrum of the Mg II feature is shown in the left hand panel of Figure 1. DeLand and Marchenko (2013) describe the OMI Mg II data set, and it is used for comparison to the new algorithm in section 3.

The Global Ozone Monitoring Experiment (GOME), launched in 1995 (Burrows et al., 1997), was the first in a series of daily measurements of the 280-nm region of the solar spectrum from ESA missions. Overlapping with GOME, the Scanning Imaging Absorption Spectrometer for Atmospheric Chartography (SCIAMACHY) observed from 2002–2012. Currently, there are three GOME-2 instruments in orbit: GOME-2A (2007 to present), GOME-2B (2012 to present), and the recently launched GOME-2C (2019 to present). These measurements are used to create the Mg II composite maintained by the University of Bremen, hereafter referred to as the "Bremen" composite, which is available online (http://www.iup.uni-bremen.de/gome/solar/MgII_composite.dat). Some details of this composite are provided in Snow et al. (2014).

The GOME, SCIAMACHY, and GOME-2 instruments have similar spectral characteristics. They use an array detector, have 0.17- to 0.3-nm spectral resolution, and use a diffuser plate (like SBUV) to measure SSI. A typical spectrum from GOME-2A is shown in Figure 1. For the GOME-2 instruments the classic definition of the Mg II index is used by first degrading the spectral resolution to 1.1 nm to match the SBUV instruments. One of the reasons for this is to reduce possible drift in the index due to changes in the instrumental response function over time. The indices published by OMI and the Bremen composite will be used as independent comparisons to the new algorithm for SOLSTICE in section 3.

2.1.3. High Spectral Resolution Observations

A second generation SOLSTICE instrument was launched on SORCE in 2003 (McClintock et al., 2005). This new instrument featured several improvements over the UARS SOLSTICE design, most importantly an increase in spectral resolution from 0.3 to 0.1 nm. Tripling the spectral resolution allows the emission cores of the Mg II feature to be fully resolved as shown in Figure 2. Also shown in Figure 2 are the red and

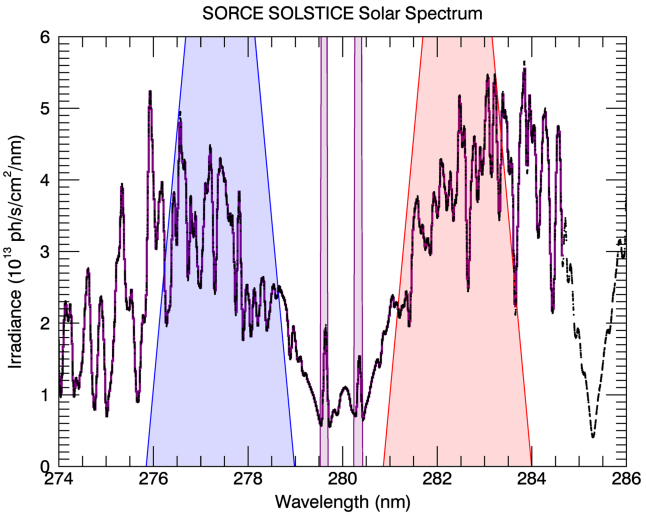

Figure 2. Typical spectrum from SORCE SOLSTICE. The red and blue shaded regions indicate the wavelength samples included in the wing weighted sums, and the purple shaded region indicates wavelengths used in the core measurement. The trapezoidal wing regions indicate the weights assigned to each wavelength to replicate Solar Ultraviolet Backscatter Radiometer-type spectral resolution (see section 3). SOLSTICE = SOLar-STellar Irradiance Comparison Experiment; SORCE = SOlar Radiation and Climate Experiment.

blue wing masks. A weighted sum of wavelengths within the mask is used to determine the denominator of the core-to-wing ratio as described in section 3

The first of the GOES-R series of operational instruments (Snow et al., 2009), which includes measurements of the Mg II index by the Extreme Ultraviolet and X-ray Sensors (EXIS), is currently in the commissioning phase. These instruments have the same spectral resolution as SORCE SOLSTICE but with higher sampling in both wavelength and time (sampling = 0.02 nm, cadence = 3 s). Once the commissioning phase is complete, the data will be available to the public, and the algorithm described here will be used to create the GOES-R data products.

The original algorithm to calculate the Mg II index from SORCE SOLSTICE was described in Snow, McClintock, Woods, et al. (2005), including comparisons to simulated lower resolution spectra based on the SOLSTICE measurement. Unlike OMI and the instruments of the Bremen composite, SOLSTICE's primary mission is to measure SSI. The primary measurement of the other instruments is atmospheric ozone, and the SSI measurement is needed as an input to the ozone retrieval. Absolute calibration of these ozone instruments is not critical since their primary measurement is a relative one. The ozone instruments generally measure SSI once per day, whereas SOLSTICE measures SSI on nearly every orbit. The benefits of higher time cadence measurements are discussed at length in both Snow, McClintock, Woods, et al. (2005) and Snow and McClintock (2005).

3. New Algorithm

In order to make the Mg II index measurements more consistent with each other, a new algorithm for computing the index has been developed for moderate and high spectral resolution data sets. The new algorithm uses weighted sums rather than curve fits and is described in detail in section 3.2. In addition to the revised algorithm for calculating the index from individual spectra, we have also developed a new method for recalibrating measurements from different instruments to a common scale (described in section 3.3).

3.1. Motivation for New Algorithm

The previous version of the algorithm for computing the core-to-wing ratio for SORCE SOLSTICE was based on fitting Gaussians to the emission cores (Snow, McClintock, Woods, et al., 2005). The technique was developed soon after the launch of SORCE when solar activity was high. Several years later when the Sun was less active and the irradiance from core lines was smaller, the Gaussian fits were not as accurate, leading to an artificially large day-to-day variance in the Mg II values. The reason the Gaussian profile is not acceptably accurate is that the instrument response to a narrow spectral input is not Gaussian (McClintock et al., 2005). This new algorithm using weighted sums rather than Gaussians greatly reduces the variation at solar minimum and brings the SORCE measurements into better agreement with the Bremen composite.

One of the challenges in linking measurements made by one instrument to another is determining the correct scaling factors. Viereck et al. (2004) used pairwise linear correlations between data sets to determine those factors. In section 3.3, we describe an alternative method of creating scaling factors that does not depend on overlapping time ranges.

de Toma et al. (1997) compared measurements from UARS SOLSTICE to SBUV/2 during the declining phase of Solar Cycle 22. At the time, there were two unique SBUV/2 data sets. One was processed by Cebula and DeLand at Goddard Space Flight Center (Cebula et al., 1992; DeLand & Cebula, 1994), while the other was processed by Donnelly at NOAA (Donnelly, 1991). De Toma et al. (1997) found that the two processing methodologies could be simulated with the higher-resolution UARS SOLSTICE data to a high level of confidence. The difference between the two methods is primarily a decision about which wavelengths were chosen for the wing measurement. De Toma et al. (1997) determined that the Donnelly method had lower noise. Snow and McClintock (2005) also simulated the two methods and came to the same conclusion: The

wavelengths chosen for the wing measurements must be far enough from the cores so that there is no contribution from core wavelengths in the wing measurement. The new algorithm discussed in section 3 takes these results into account.

Another conclusion of de Toma et al. (1997) was that the higher-resolution UARS SOLSTICE measurement captured more solar variability than the SBUV/2 observation. Snow, McClintock, Woods, et al. (2005) made similar comparisons using SORCE SOLSTICE data, and they also found that the higher spectral resolution instrument captured more solar variability. The new algorithm for computing the Mg II index also takes this into account. Convolving these higher spectral resolution instruments with a wider response function is useful for scaling (section 3.3), but it reduces the repeatability of the measurement (Snow & McClintock, 2005; Snow, McClintock, Woods, et al., 2005); that is, random noise in the spectrum on the edges of the core features is a large contribution to the total uncertainty of the index. The statistical uncertainty of those nearby wavelengths is large because the signal levels are low, so excluding them from the numerator of the core-to-wing ratio leads to a significant improvement in the uncertainty of the Mg II index.

In developing the new algorithm, we also revisited the assumption that instrument degradation corrections cancel out in the core-to-wing ratio. Section 4 quantifies the effect of long-term degradation on the index time series.

3.2. Weighted Sums

There are two quantities that need to be calculated in the core-to-wing ratio, namely, the core and the wings. As described in Snow, McClintock, Woods, et al. (2005), a very stable method of determining the wing irradiance values is to smooth the spectrum to the spectral resolution of the classic SBUV, that is, a 1.1-nm triangular band pass. If the spectrum is sampled on a regular wavelength grid, the triangular smoothing is mathematically identical to a weighted sum. The advantage of the weighted sum algorithm is that in the case of an array detector, individual pixels can have their weights adjusted without changing the contribution of other pixels. For an instrument such as SORCE SOLSTICE with a single photomultiplier tube detector (McClintock et al., 2005), this algorithm can still be applied to the irradiance samples collected at each grating step during a spectral scan. In fact, the weighted sum algorithm can be applied to nearly any instrument design and will be implemented on the next generation of Mg II index instruments on the GOES-R series (Eparvier et al., 2009; Snow et al., 2009).

The weighting for the wing measurements are shown in Figure 2 as shaded areas. The relative weights for each wavelength are indicated by the height of the shaded region. In each case, the weighting function is a trapezoid with values ranging from zero to one. The wavelengths included in the core sums are all equally weighted.

Our analysis starts with the publicly available, high-resolution daily average spectrum available on the SORCE web page at http://lasp.colorado.edu/sorce/data as yearly NetCDF files. These data are also available through the LASP Interactive Solar Irradiance Datacenter at the website (http://lasp.colorado.edu/lisird). The way this data product is generated is that all of the calibrated, Level 2, measurements obtained over a 24-hr period are sorted by wavelength. The individual spectral scans collected each orbit by SORCE SOLSTICE have a spacing of 0.033 nm. Some scans in this wavelength region go from shorter wavelengths to longer ones, while others scan in the reverse direction. Additional scans of just the 280-nm region can occur throughout the orbit. The net effect of this variety of scan types is that Doppler shifts will offset the regular wavelength grid from one scan to another. When all scans in a 24-hr period are considered together, the individual offsets result in higher wavelength sampling than can be achieved on any single scan. We take advantage of this improved sampling by fitting a high-order basis spline to all the irradiance samples as a function of wavelength. The data pipeline evaluates the spline function on a regular grid with 0.025-nm spacing. This spacing was determined to preserve the spectral content of the data.

The development of the algorithm for calculating the EXIS Mg II index is fairly mature (Snow et al., 2018), and we have leveraged that development to improve the SORCE SOLSTICE Mg II data product. The new algorithm evaluates the SOLSTICE daily spline onto the wavelength grid sampled by EXIS and uses the same weighting functions for the core and wings for both instruments. These weighting functions are defined to simulate a 1.1-nm spectral resolution for the wings and to capture all of the core irradiance. As described in Snow et al. (2018), the weighted sums are calculated from the EXIS observations as part of the standard data processing pipeline.

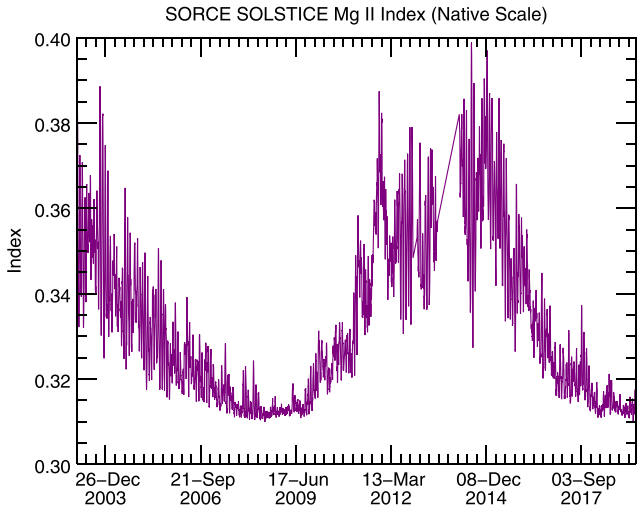

Figure 3. Revised Mg II index from SORCE SOLSTICE using the new algorithm. SOLSTICE = SOLar-STellar Irradiance Comparison Experiment; SORCE = SOlar Radiation and Climate Experiment.

Figure 3 shows the results of the new algorithm applied to the full mission of SORCE SOLSTICE. Starting in 2003, SORCE SOLSTICE has observed nearly every day with one notable exception. In mid-2013, the spacecraft went into safe hold due to degradation of the battery system. It resumed daily operations in early 2014.

3.3. Self-Scaling

The value of any individual Mg II data set is greatly increased if it can be connected to other instrument data records to create a longer-term composite. The primary challenge in creating such a composite is determining scaling factors from one instrument to another (Viereck et al., 2004). Each instrument team has defined its own algorithm for producing the best proxy from their measurement (e.g., Snow, McClintock, Woods, et al., 2005). Sometimes, there is more than one algorithm applied to the same raw data from different teams: Donnelly (1991) versus DeLand and Cebula (1994).

The linear correlation between data sets used by Viereck et al. (2004) assumes that there are no long-term trends due to instrument artifacts in any of the records. That scaling scheme picks one data set as a reference, and then daisy chains subsequent time domains onto the previous data set. If there is an uncorrected trend in any data set in the chain, that trend will influence all later records. Section 4 will quantify the magnitude of residual degradation on the index time series.

One way to avoid the possibility of trend errors in one data set being propagated to subsequent data sets in a composite is to scale each record individually and independently to a defined standard spectral resolution. In this case, we have chosen an instrument profile with a 1.1-nm triangular band pass as the standard. It will allow the creation of a new composite. A linear correlation such as Viereck et al. (2004) of measurements over some time interval is used to scale the daily native-scale index produced by the instrument team to the daily standard index produced by convolving each observed spectrum with a 1.1-nm triangular profile. Since this scaling factor uses the same spectrum (at native spectral resolution and at low resolution), we refer to this method as self-scaling. The time interval chosen in this analysis was 1 year. Figure 4 shows the result of such a scaling for the SORCE SOLSTICE and GOME-2A data sets as an example.

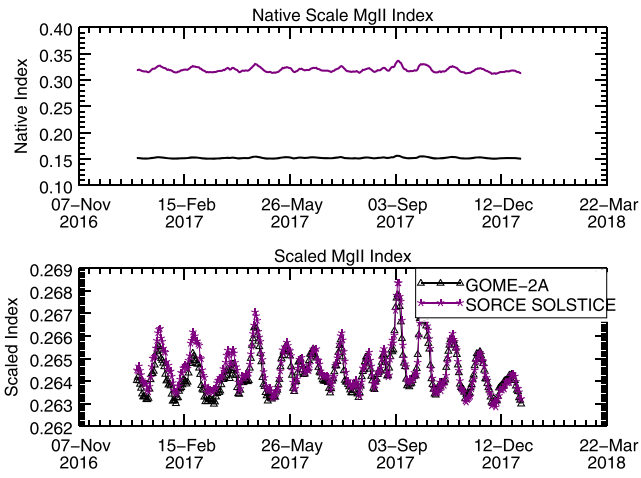

Figure 4. Sample self-scaling result. The top panel shows the Mg II index from SORCE SOLSTICE and GOME-2A on their native scales. GOME-2A's values are near 0.15 (black), and SOLSTICE's native scale is near 0.3 (purple). In the lower panel, the GOME-2A and SORCE SOLSTICE spectra are independently scaled to 1.1-nm spectral resolution. The time series for 1 year are shown as an example of the result of self-scaling. GOME = Global Ozone Monitoring Experiment; SORCE = SOlar Radiation and Climate Experiment; SOLSTICE = SOLar-STellar Irradiance Comparison Experiment.

Since the self-scaling technique does not use information from other data sets, the Mg II index from different missions is now completely independent measurements. Figure 5 shows the ratio of the Bremen composite and OMI to SORCE SOLSTICE. The previous version of the SORCE SOLSTICE Mg II index deviated from the Bremen composite starting in 2006 (Snow et al., 2014). The new version of the SOLSTICE data has no trend with respect to either OMI or the Bremen composite; however, a small trend may exist after the SORCE safehold event in mid-2013. The batteries on SORCE had degraded to the point that the spacecraft could not survive an eclipse without the battery voltage falling below a critical threshold. Eventually, the LASP mission operations team was able to recover the spacecraft and change the operational mode. SORCE can now take data on nearly every orbit. The new operational mode has changed the way that SOLSTICE acquires calibration data to correct for long-term degradation, and this may have a residual effect on the current version of the Mg II index. Section 4 will discuss this effect in detail.

4. Effects of Degradation

Heath and Schlesinger (1986) made the assumption that instrument artifacts such as long-term degradation cancel out in the proxy. As measurements achieved higher signal-to-noise ratios, the requirements for

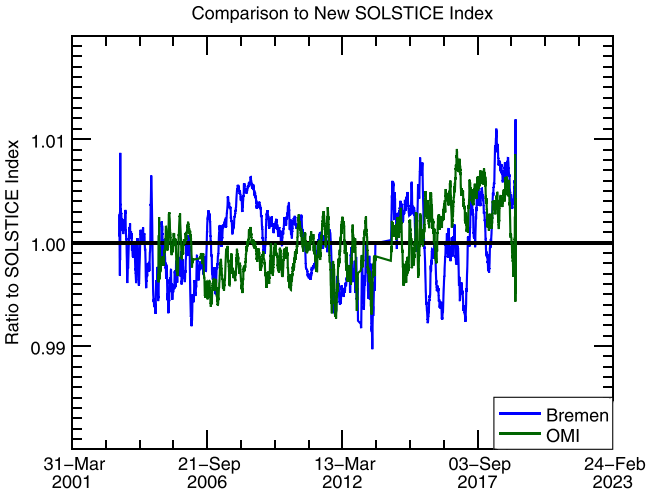

Figure 5. Ratio of Bremen composite and OMI Mg II indices to the new SORCE SOLSTICE index. Data sets have been smoothed with a 27-day running mean. Compare to Figure 6 of Snow et al. (2014). OMI = Ozone Monitoring Instrument; SOLSTICE = SOLar-STellar Irradiance Comparison Experiment.

long-term stability have become more strict. In this section we will quantify the effect of instrument degradation on the calculated proxy. As an example, we will use data from SORCE SOLSTICE both with and without correction for long-term degradation. The SOLSTICE degradation correction is based on observations of bright stars and a correction for the difference in solar and stellar viewing geometries (Snow, McClintock, Rottman, et al., 2005). There is some indication in the literature that there is still uncorrected degradation in the SORCE SOLSTICE SSI; see, for example, Ermolli et al. (2013). The purpose of using these two data sets is to quantify the impact of degradation on the Mg II index time series, so comparing uncorrected data to partially corrected data will still show the effect of the residual degradation. If all degradation factors canceled out in the Mg II index, then the two cases would show the same final result.

Let us assume that instrument degradation is a function of time and wavelength, with a multiplicative degradation factor with linear wavelength dependence near 280 nm given by

$$d(\lambda, t) = d_0(t) + d_1(t)(\lambda - \lambda_0), \tag{2}$$

where $d_0(t)$ is an arbitrary function of time that yields the degradation at 280 nm and λ_0 is 280 nm. Here $d_0(t = 0) = 1$ and $d_1(t = 0) = 0$. Figure 6 shows the normalized irradiance for SORCE SOLSTICE as a function of time since the beginning of its mission both with and without degradation corrections applied. The degradation correction for SORCE SOLSTICE is described in Snow, McClintock, Rottman, et al. (2005). It includes observations of stable stars and a correction for the solar/stellar viewing geometry. The uncertainty in this correction is about 0.3% per year.

The three wavelength regions plotted are the red and blue wings (red and blue diamonds) and a region between the two emission cores (279.8–280.1 nm). This intercore region has less solar variability than either core but does still have some variation with the solar cycle. This is particularly obvious in the lower panel of Figure 6. In the upper panel, the instrument degradation dominates the solar cycle.

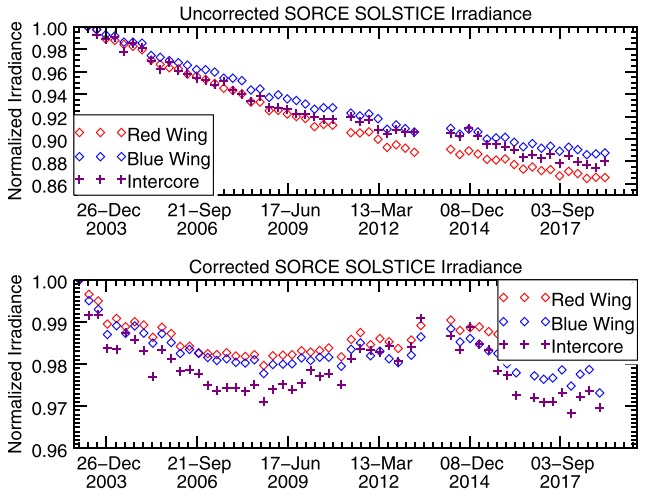

Figure 6. Normalized signal in SORCE SOLSTICE wings and intercore region. The upper panel shows the uncorrected irradiance as a function of time for three selected wavelength regions. The lower panel shows the irradiance after being corrected for degradation. Red and blue diamonds represent the two wing sums, and the purple plus signs are the average irradiance between the two emission cores. For clarity, one time sample every 100 days is shown. SOLSTICE = SOLar-STellar Irradiance Comparison Experiment; SORCE = SOlar Radiation and Climate Experiment.

After the safehold event in 2013, the slope of the degradation changed significantly. The operation of the satellite changed, and we are still developing a new degradation correction for the post-2013 data. We are optimistic that the version 17 SOLSTICE data product will improve the accuracy of the SSI measurement throughout the SORCE mission. The impact of the changed rate of degradation will be discussed later in this section.

The time series of the normalized intercore values is dominated by solar cycle variation after correction for degradation (lower panel of Figure 6). The magnitude of the variation of the intercore is somewhat larger than the variation of the wings, but they are of similar magnitude. The small amount of variability shown in the wings in the lower panel of Figure 6 is due to variability in the cores of the Fraunhofer lines.

Although the SSI time series shown in Figure 6 have been corrected for known sources of degradation, the fact that the irradiances during the declining phase of Solar Cycle 23 early in the mission are higher than the maximum of Solar Cycle 24 indicates that there is likely still some uncorrected long-term degradation in the current version of the SOLSTICE data product (version 16). Ermolli et al. (2013) discuss the magnitude of the uncorrected degradation in comparison to other measurements and models. The lower panel of Figure 6 puts an upper limit of the missing degradation correction at about 1% over a solar cycle. Analysis of new calibration measurements after the SORCE safehold event will further improve the degradation correction throughout the mission.

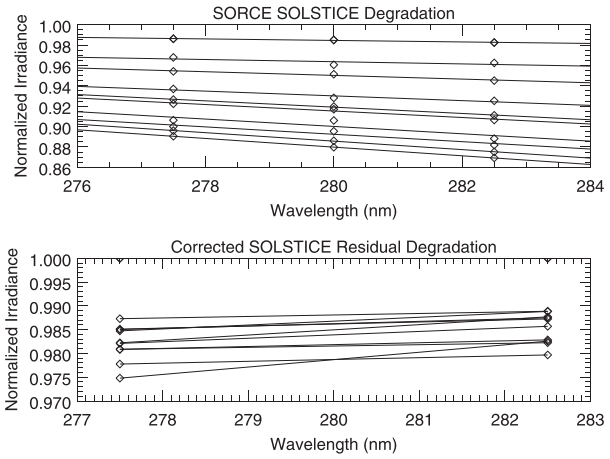

Figure 7. Degradation for wings and intercore as a function of wavelength. The normalized irradiances shown in Figure 6 are plotted here versus wavelength. Only every fifth time sample is plotted for clarity. SOLSTICE = SOLar-STellar Irradiance Comparison Experiment; SORCE = SOlar Radiation and Climate Experiment.

Is the assumption that the degradation function is linear with wavelength at any given time a good one? Figure 7 shows the same data as Figure 6 but instead plotted as a function of wavelength. The three values for each date (red wing, blue wing, and intercore) are shown as a function of wavelength with a linear fit in the upper panel. In the upper panel of Figure 7, the data have not been corrected for degradation, while in the lower panel, all currently known corrections for instrument degradation (Snow, McClintock, Rottman, et al., 2005) have been applied.

These linear fits show the estimation of d_0 and d_1 in equation (2). The value of the line at 280 nm for each day is d_0, and the slope of the line is d_1. If the degradation had been perfectly corrected, d_0 would be a constant, and d_1 would be 0.

In the lower panel of Figure 7, only the two wings are plotted since the intercore's time series is dominated by solar variability. While it is true that we are fitting a line to only three points on each day for the uncorrected case, the assumption that instrument degradation is approximately linear over a few nanometers seems reasonable. In the general case where $d(\lambda, t)$ is more complex than shown in equation (2), we would be using only the first two terms of a Taylor expansion of the true degradation function.

The Magnesium II proxy in general is the ratio of the core irradiance divided by the wing irradiance times some normalization constant; that is,

$$P_{\mathrm{MgII}} = A\frac{C_h + C_k}{W_b + W_r}, \tag{3}$$

where A is a constant, C_h and C_k are the irradiances of the cores, and W_r and W_b are the irradiances of the red and blue wings. While the magnitude of the solar variability in the cores is much larger than in the wings, the wings do show some measurable change over the solar cycle.

The C and W terms are functions of time that will vary due to solar variability. In this notation, C and W include only solar variation, not degradation. The degradation terms (d_0 and d_1) are noted explicitly. Using the degradation function of equation (2) and making the simplification that all the core irradiance comes from λ_0, the proxy can be expressed as follows:

$$P_{\mathrm{MgII}}(t) = A\frac{C_h d(t,\lambda_0) + C_k d(t,\lambda_0)}{W_b d(t,\lambda_0 - \Delta\lambda) + W_r d(t,\lambda_0 + \Delta\lambda)}. \tag{4}$$

Equation (4) simplifies to

$$P_{\mathrm{MgII}}(t) = A\frac{d_0(C_h + C_k)}{d_0(W_b + W_r) + d_1\Delta\lambda(W_r - W_b)} \tag{5}$$

If $d_1\Delta\lambda(W_r - W_b)$ is small compared to $d_0(W_b + W_r)$, then the second term can be neglected, and d_0 cancels out. In that case, equation (5) simplifies to equation (3) as assumed in Heath and Schlesinger (1986). On the other hand, if $d_1\Delta\lambda(W_r - W_b)$ cannot be neglected, then we can estimate the magnitude of the impact of degradation over time as follows. The ratio of the proxy at $t = 0$ to any time t is given by

$$\frac{P_{\mathrm{MgII}}(0)}{P_{\mathrm{MgII}}(t)} = \left(A\frac{C_h + C_k}{W_b + W_r}\right) / \left(A\frac{d_0(C_h + C_k)}{d_0(W_b + W_r) + d_1\Delta\lambda(W_r - W_b)}\right), \tag{6}$$

which simplifies to

$$\frac{P_{\mathrm{MgII}}(0)}{P_{\mathrm{MgII}}(t)} = 1 + \left(\frac{d_1\Delta\lambda}{d_0}\right)\left(\frac{W_r - W_b}{W_r + W_b}\right). \tag{7}$$

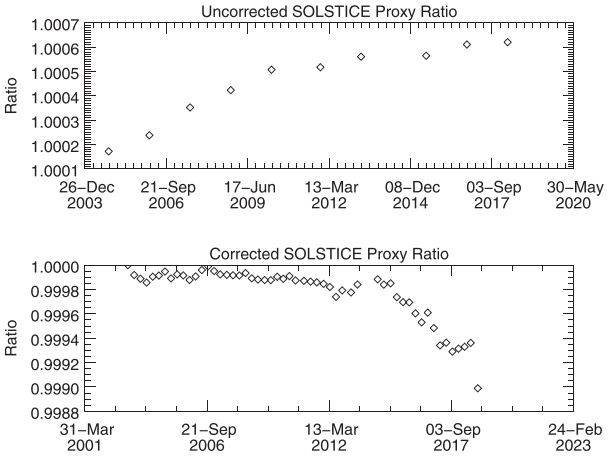

Figure 8. The ratio of the Mg II proxy as a function of time for SORCE SOLSTICE before and after applying all known degradation corrections. The top panel shows the results for uncorrected data, while the lower panel shows the results after correction for long-term degradation. This is the quantity $1 + \left(\frac{d_1\Delta\lambda}{d_0}\right)\left(\frac{W_r - W_b}{W_r + W_b}\right)$ as derived in equation (7). SOLSTICE = SOLar-STellar Irradiance Comparison Experiment; SORCE = SOlar Radiation and Climate Experiment.

The results shown in Figure 8 are the magnitude of instrument trends in the Mg II index caused by instrument artifacts. Without correction for long-term degradation, the estimated drift in the Mg II index would be 0.0005 over a solar cycle. The native-scale change of the SOLSTICE Mg II index over the solar cycle is 0.08, so the estimated drift using uncorrected data would be 0.6% of the solar cycle amplitude. Using corrected data, the drift from 2003 to 2013 is only 0.0001, or about one fifth as large as for uncorrected data (i.e., less than 0.1% of the solar cycle amplitude).

Note that after 2013, the lower panel of Figure 8 shows a precipitous drop in the estimated drift. This corresponds to the resumption of spacecraft operations after the 6-month safehold. It could indicate that the degradation correction after 2013 is poor in this part of the spectrum. The effect is also seen in the lower panel of Figure 6 where the separation between the red and blue wings grows with time after 2013.

5. Discussion

High-resolution spectral measurements have the capability of measuring more short-term solar variability than lower-resolution instruments (de Toma et al., 1997; Snow & McClintock, 2005; Snow, McClintock, Woods, et al., 2005). On longer timescales, that is, solar cycle and multidecadal, measurements from all instruments converge (Snow, McClintock, Woods, et al., 2005). The low- and moderate-resolution instruments typically measure the incoming SSI only once per day, while higher-resolution instruments are used to make higher time cadence measurements (Snow, McClintock, Woods, et al., 2005; Snow et al., 2009).

The method of calculating the Mg II index from SORCE SOLSTICE as described in Snow, McClintock, Woods, et al. (2005) produced a daily value at solar minimum with a fairly large day-to-day variance (Snow et al., 2014). It was difficult to determine if this was true solar variability or merely an artifact of the data processing algorithm. Recent investigation using the newly launched GOES-R EXIS instrument (Snow et al., 2018) confirmed that the Gaussian modeling of the observed emission cores was not producing good fits. The EXIS instrument (Snow et al., 2009) has the same spectral resolution as SORCE SOLSTICE but higher sampling in both wavelength and time. We have adopted a simpler reduction strategy for both instruments: weighted sums for both cores and wings.

In addition to the new algorithm for processing each individual measurement, we have also developed a new way of scaling the time series to a common standard. Knowing the parameters of each instrument (resolution and sampling), it is easy to convolve a spectrum to match the classic low-resolution observation as described in Heath and Schlesinger (1986). Rather than calculate the linear correlation of each instrument team's reduced data to the reduced data of another instrument (Viereck et al., 2004), we do the linear correlation of the team's method to the classical calculation. Thus, each instrument is scaled to a common standard without the need to select a custom time period of overlap. More importantly, if any one version of a data set has an uncorrected long-term trend, that trend will not be communicated to any other components of a long-term composite. We will use this new data set in a new composite.

Finally, we have analyzed the impact of instrument degradation on the Mg II index. As first described in Heath and Schlesinger (1986), one of the main reasons that the core-to-wing ratio is a good proxy is because it is insensitive to instrument artifacts. We have calculated the residual effect of a degradation function that is approximately linear in wavelength near 280 nm. Our conclusion is that degradation-corrected data are better but that uncorrected data still produce a highly accurate Mg II index. As a test case, we found that uncorrected SORCE SOLSTICE data produced a long-term error in the Mg II index that is less than 1% of the solar cycle amplitude (0.6%). Using corrected data, that error decreases by a factor of 5 to about 0.1% of the solar cycle amplitude.

Acknowledgments
This work was supported by NASA Grant NNX15AI53G (SSIAMESE) as part of the Solar Irradiance Science Team (SIST) program. The data set described here can be downloaded from the LASP Interactive Solar Irradiance Datacenter (LISIRD; http://lasp.colorado.edu/lisird). SORCE SOLSTICE version 16 was used in this analysis. The authors would like to thank the two anonymous reviewers who helped improve the clarity of the manuscript.

References

Burrows, J., Buchwitz, M., Rozanov, V., Weber, M., Richter, A., Ladstäter-Weißenmayer, A., & Eisinger, M. (1997). The global ozone monitoring experiment (GOME): Mission, instrument concept. & first scientific results. In T.-D. Guyenne, & D. Danesy (Eds.), *Third ERS Symposium on Space at the Service of our Environment* (Vol. 414, pp. 585): Florence, Italy: ESA special publication.

Cebula, R., DeLand, M., & Schlesinger, B. (1992). Estimates of solar variability using the solar backscatter ultraviolet (SBUV) 2 Mg II index from NOAA 9 satellite. *Journal of Geophysical Research*, *97*, 11,613–11,620. https://doi.org/10.1029/92JD00893

de Toma, G., White, O., Knapp, B., Rottman, G., & Woods, T. (1997). Mg II core-to-wing index: Comparison of SBUV2 and SOLSTICE time series. *Journal of Geophysical Research*, *102*, 2597–2610. https://doi.org/10.1029/96JA03342

DeLand, M., & Cebula, R. (1994). Comparisons of the Mg II index products from the NOAA-9 and NOAA-11 SBUV/2 instruments. *Solar Physics*, *152*, 61–68. https://doi.org/10.1007/BF01473184

DeLand, M., Cebula, R., & Hilsenrath, E. (2004). Observations of solar spectral irradiance change during cycle 22 from NOAA-9 solar backscattered ultraviolet model 2 (SBUV/2). *Journal of Geophysical Research*, *109*, D06304. https://doi.org/10.1029/2003JD004074

DeLand, M., & Marchenko, S. (2013). The solar chromospheric Ca and Mg indices from Aura OMI. *Journal of Geophysical Research: Atmospheres*, *118*, 3415–3423. https://doi.org/10.1002/jgrd.50310

Donnelly, R. (1991). Solar UV spectral irradiance variations. *Journal of Geomagnetism and Geoelectricity*, *43*(supplement series 2), 835–842. https://doi.org/10.5636/jgg.43.Supplement2_835

Dudok de Wit, T., Kretzschmar, M., Lilenstein, J., & Woods, T. (2009). Finding the best proxies for the solar UV irradiance. *Geophysical Research Letters*, *36*, L10107. https://doi.org/10.1029/2009GL037825

Eparvier, F., Crotser, D., Jones, A., McClintock, W., Snow, M., & Woods, T. (2009). The extreme ultraviolet sensor (EUVS) for GOES-R. *Proceedings of the SPIE*, *7438*(743804), 8. https://doi.org/10.1117/12.826445

Ermolli, I., Matthes, K., Dudok de Wit, T., Krivova, N., Tourpali, K., Weber, M., et al. (2013). Recent variability of the solar spectral irradiance and its impact on climate modelling. *Atmospheric Chemistry & Physics*, *13*, 3945–3977. https://doi.org/10.5194/acp-13-3945-2013

Floyd, L., Prinz, D., Crane, P., Herring, L., & Brueckner, G. (1999). SUSIM UARS measurements of solar UV irradiance. *Advances in Space Research*, *24*, 225–228.

Floyd, L., Tobiska, W. K., & Cebula, R. (2002). Solar uv irradiance, its variation, and its relevance to the Earth. *Advances in Space Research*, *29*, 1427–1440.

Frederick, J., Heath, D., & Cebula, R. (1986). Instrument characterization for the detection of long-term changes in stratospheric ozone—An analysis of the SBUV/2 radiometer. *Journal of Atmospheric and Oceanic Technology*, *3*, 472. https://doi.org/10.1175/1520-0426(1986)003<0472:ICFTDO>2.0.CO;2

Haigh, J. (1994). The role of stratospheric ozone in modulating the solar radiative forcing of climate. *Nature*, *370*, 544–546. https://doi.org/10.1038/370544a0

Heath, D., Krueger, A., Roeder, H., & Henderson, B. (1975). The solar backscatter ultraviolet and total ozone mapping spectrometer SBUV/TOMS for Nimbus G. *Optical Engineering*, *14*, 323–331. https://doi.org/10.1117/12.7971839

Heath, D., & Schlesinger, B. (1986). The Mg 280-nm doublet as a monitor of changes in solar ultraviolet irradiance. *Journal of Geophysical Research*, *91*, 8672–8862. https://doi.org/10.1029/JD091iD08p0872

Levelt, P., van den Oord, G., Dobber, M., Malkki, A., Visser, H., de Vries, J., & Stammes, P. (2006). The Ozone Monitoring Instrument. *IEEE Transactions on Geoscience and Remote Sensing*, *44*, 1093–1101. https://doi.org/10.1109/TGRS.2006.872333

McClintock, W., Rottman, G., & Woods, T. (2005). Solar-Stellar Irradiance Comparison Experiment II (SOLSTICE II): Instrument concept and design. *Solar Physics*, *230*, 225–258. https://doi.org/10.1007/s11207-005-7432-x

Rottman, G. (2005). The SORCE mission. *Solar Physics*, *230*, 7–25. https://doi.org/10.1007/s11207-005-8112-6

Rottman, G., Woods, T., & Sparn, T. (1993). Solar-stellar irradiance comparison experiment 1. I—Instrument design and operation. *Journal of Geophysical Research*, *98*, 10,667–10,677. https://doi.org/10.1029/93JD00462

Snow, M., Machol, J., Eparvier, F., Jones, A., McClintock, W., & Woods, T. (2018). Magnesium II Index measurements from SORCE SOLSTICE and GOES-16 EUVS. *Proceedings of the International Astronomical Union*, *13*(S340), 167–168. https://doi.org/10.1017/S174392131800128X

Snow, M., & McClintock, W. (2005). High time cadence solar Magnesium II index monitor. *Proceedings of the SPIE*, *5901*, 354–365. https://doi.org/10.117/12.617044

Snow, M., McClintock, W., Crotser, D., & Eparvier, F. (2009). EUVS-C: The measurement of the magnesium II index for GOES-R EXIS. *Proceedings of the SPIE*, *7438*(743803), 10. https://doi.org/10.1117/12.828566

Snow, M., McClintock, W., Rottman, G., & Woods, T. (2005). Solar Stellar Irradiance Comparison Experiment II (SOLSTICE II): Examination of the solar stellar comparison technique. *Solar Physics*, *230*, 295–324. https://doi.org/10.1007/s11207-005-8763-3

Snow, M., McClintock, W., Woods, T., White, O., Harder, J., & Rottman, G. (2005). The Magnesium II index from SORCE. *Solar Physics*, *230*, 325.

Snow, M., Weber, M., Machol, J., Viereck, R., & Richard, E. (2014). Comparison of Magnesium II core-to-wing ratio observations during solar minimum 23/24. *Journal of Space Weather and Space Climate*, *4*(A04), 6. https://doi.org/10.1051/swsc/2014001

Thuillier, G., Bolsée, D., DeLand, M., Melo, S., Schmutz, W., & Shapiro, A. (2012). The solar spectral irradiance as a function of the Mg II index for atmosphere and climate modelling. *Solar Physics*, *277*, 245–266. https://doi.org/10.1007/s11207-011-9912-5

Thuillier, G., & Bruinsma, S. (2001). The Mg II index for upper atmosphere modelling. *Annales Geophysicae*, *19*, 219–228. https://doi.org/10.5194/angeo-19-219-2001

Viereck, R., Floyd, L., Crane, P., Woods, T., Knapp, B., Rottman, G., et al. (2004). A composite Mg II index spanning from 1978 to 2003. *Space Weather*, *2*, S10005. https://doi.org/10.1029/2004SW00084